Journal of Magnetic Resonance 193 (2008) 119–126

Contents lists available at ScienceDirect

Journal of Magnetic Resonance

journal homepage: www.elsevier.com/locate/jmr

Stochastic Liouville equation studies of FT-EPR spectra of singlet–triplet mixing photo-chemically generated radical pair system

Ryuji Hanaishi *

Gappo 2-8-25-203, Aomori City, Aomori 030-0902, Japan

ARTICLE INFO

Article history:
Received 3 October 2007
Revised 27 March 2008
Available online 29 April 2008

Keywords:
Stochastic Liouville equation
FT-EPR
Radical pair
CIDEP

ABSTRACT

A stochastic Liouville equation (SLE) was numerically solved to obtain pulsed Fourier-transform (FT) EPR spectra on a radical pair system created in a photo-induced chemical reaction. Numerical calculations were applied to the photo-chemical reaction of deuterated acetone and 2-propanol at low temperatures. In this reaction system, the antiphase structures of the EPR signals, so called spin-correlated radical pair (SCRP) signals of two identical isopropyl ketyl radicals and spin-polarized free isopropyl ketyl radicals were observed by FT-EPR and continuous wave time-resolved (CW TR) EPR techniques. In the present work, FT-EPR spectra of the antiphase structure signals of the radical pair themselves as well as spin-polarized free radical signals were simulated. Additionally, rising behavior of free radical signals polarized by the radical pair mechanism (RPM) was also clarified. Furthermore two-dimensional (2D) FT-EPR nutation spectra were simulated in the both cases with and without the radical pairs by the use of SLE. In these simulations, strong DC components in the nutation frequency dimension, were well reproduced as was obtained in experiments. It was shown that relaxation during the microwave pulse was essential for the appearance of the DC components.

1. Introduction

The time-resolved (TR) and pulsed Fourier-transform (FT) EPR have widely been used to obtain much information about reaction mechanisms and spin dynamics on the photo-chemically generated free radicals and intermediate radical pairs [1]. One of the great abilities of EPR is to characterize directly the molecular structures of intermediate radicals and radical pairs as well as their occurring and decays from the initial stages of the photo-chemical reactions.

Concerning on spin dynamics, detailed theories for the chemically induced dynamic electron and nuclear polarization (CIDEP and CIDNP) were proposed [2–4] in 1970s based on stochastic Liouville equation (SLE). In the field of EPR, the SLE application to analyses of spectra of antiphase structures of the EPR signals of the radical pair systems, that were so called spin-correlated radical pair (SCRP) signals, generated in photo-chemical reactions were reported [5]. In this work [5] EPR signals polarized by ST_0 mixing radical pair mechanism (RPM) and the antiphase signals were successfully simulated for the first time. Then epoch-making discoveries on mechanisms of origins of antiphase EPR signals concerning radical pair systems were made by Neufeld and Pedersen [6,7].

The present author considers that EPR simulations in terms of the SLE method are very useful to make experimentally obtained information more quantitatively as well as more in details for chemical reaction and spin dynamic systems. They are also useful to investigate the spin dynamics at earlier stage than experimentally obtained because the theoretical calculations are not affected by instrumental deadtimes.

The CIDEP signals of antiphase structures of the radical pairs obtained by pulsed FT-EPR measurements have been reported for various reaction systems [8–10]. Previously, the present author proposed the two-dimensional (2D) FT-EPR nutation method to studies of the radical pairs [11–14]. In these studies, simulations of the 2D spectra were attempted by using an averaged single exchange interaction parameter. In the theory of SLE, stochastic modulations of exchange interactions within radical pairs can be taken into account. However, no SLE studies have been attempted for the radical pairs observed by the FT-EPR, although SLE and FT-EPR measurements are both treated in the same time domain.

In this paper, the author puts X-band pulsed FT-EPR spectra of a photo-induced chemical reaction of deuterated acetone and 2-propanol system at low temperatures in the sights of the SLE simulation. On this reaction system, extensive CW TR-EPR and FT-EPR studies have been reported [9,15–20]. In this reaction, via photo-excited triplet state of acetone, two isopropyl ketyl radicals are formed by the excited acetone's hydrogen abstraction from 2-propanol of solvent, giving the antiphase EPR structures with identical two isopropyl ketyl radicals and free isopropyl ketyl radicals accompanied with CIDEP. The present paper describes the SLE simulations of one-dimensional (1D) FT-EPR signals of the radical pairs

* Fax: +81 17 736 5419.
E-mail address: stein.ryuji@nifty.ne.jp

1090-7807/$ - see front matter © 2008 Elsevier Inc. All rights reserved.
doi:10.1016/j.jmr.2008.04.032

systems. By means of these simulations, some parameters in the SLE are determined.

Additionally, rising behaviors of the EPR signals caused by the ST_0 mixing RPM are clarified for the first time. It is shown that predictions from the ST_0 mixing RPM theory proposed by Adrian and Monchick [21] deviate from the results of SLE when diffusions of the radical pairs are largely inhibited, as Shushin showed [22,23].

Finally two-dimensional (2D) FT-EPR nutation spectra are simulated in the both cases under presence and absence of radical pairs, and effects of spin relaxation are discussed. The consideration of the 2D spectra are essential from the view point that the EPR spectra of the radical pairs should strongly depend on the excitation microwave filed strength as suggested by the coherent effect model [6,7] and that strong microwaves are applied in the case of the FT-EPR.

2. Theory

If the exchange interaction between the radicals in radical pairs of inter-radical distance r is taken to be $J(r)$, the spin Hamiltonian $H_0(r)$ in the static magnetic field B_0 is written under the laboratory frame as follows:

$$H_0(r) = g_a\mu_B B_0 S_{az} + g_b\mu_B B_0 S_{bz} + \sum_j a_j \mathbf{S}_a\mathbf{I}_\mathbf{j} + \sum_k a_k \mathbf{S}_b\mathbf{I}_\mathbf{k} - J(r)\left(\frac{1}{2} + 2\mathbf{S}_a\mathbf{S}_b\right). \quad (1)$$

Here, the other symbols have usual meanings. By the use of the high field approximation and if only the ST_0 mixing is considered, $H_0(r)$ is rewritten as

$$H_0(r) = g_a\mu_B B_0 S_{az} + g_b\mu_B B_0 S_{bz} + \sum_j a_j S_{az} I_{jz} + \sum_k a_k S_{bz} I_{kz} - J(r)\left(\frac{1}{2} + 2\mathbf{S}_a\mathbf{S}_b\right). \quad (2)$$

In the rotating flame Eq. (2) becomes

$$H_0(r)_{\mathrm{rot}} = \omega_a S_{az} + \omega_b S_{bz} - J(r)\left(\frac{1}{2} + 2\mathbf{S}_a\mathbf{S}_b\right), \quad (3)$$

where ω_a is resonance offset of radical a with the corresponding hyperfine state.

The spin Hamiltonian expressing the influence of a microwave excitation pulse along with $-y$ axis is written in the rotating flame as

$$H_{1,\mathrm{rot}} = -g_a\mu_B B_1 S_{ay} - g_b\mu_B B_1 S_{by} \quad (4)$$

$$= -\omega_{1a} S_{ay} - \omega_{1b} S_{by}. \quad (5)$$

The SLE is a partial differential equation and in the case of electrically neutral radical pairs it is written as

$$\frac{\partial\rho(r,t)}{\partial t} = -\mathrm{i}\left[H(r)_{\mathrm{rot}}, \rho(r,t)\right] + D\Gamma_r(r)\rho(r,t) + \mathrm{R}\rho(r,t). \quad (6)$$

In Eq. (6), $H(r)_{\mathrm{rot}}$ expresses the spin Hamiltonian in the rotating flame, $\rho(r,t)$ is the spin density operator depending on time and radical–radical distance r, D is the diffusion coefficient, and Γ_r and R are the diffusion and the relaxation super operators, respectively.

If one defines as $\hat{\rho}(r,t) = r\rho(r,t)$, SLE (6) becomes

$$\frac{\partial\hat{\rho}(r,t)}{\partial t} = -\mathrm{i}\left[H(r)_{\mathrm{rot}}, \hat{\rho}(r,t)\right] + D\Gamma_r(r)\hat{\rho}(r,t) + \mathrm{R}\hat{\rho}(r,t). \quad (7)$$

Then the distance-dependent diffusion term becomes simpler and it is expressed by

$$\Gamma_r\hat{\rho}(r,t) = \partial^2\hat{\rho}(r,t)/\partial r^2. \quad (8)$$

The Redfield relaxation is taken into consideration, but both of Boltzmann-distributed spin density operators and any longitudinal relaxations to them are neglected. These neglect are adequate because the radical pairs lie in the spin-correlated states and radical pairs with thermally equilibrated spin states have not been discovered. The magnetization of radical pairs is set to relax according to the relaxation super operator in the Liouville space as follows:

$$\mathbf{R} = \mathbf{R_a}\otimes\mathbf{1_b} + \mathbf{1_a}\otimes\mathbf{R_b}, \quad (9)$$

and

$$\begin{array}{cc} & \begin{array}{cccc} \alpha\alpha & \alpha\beta & \beta\alpha & \beta\beta \end{array} \\ \mathbf{R_a} = & \begin{bmatrix} -1/T_{1a} & & & \\ & -1/T_{2a} & & \\ & & -1/T_{2a} & \\ & & & -1/T_{1a} \end{bmatrix} \end{array} \quad (10)$$

where T_{1a} and T_{2a} are the longitudinal and transverse relaxation times of radical a, respectively.

3. Simulation method

In order to solve SLE numerically, the super operator and the density operator are transformed into discrete matrix and vector, respectively, as already described [2–4]. For calculations of electron and nuclear spin polarizations caused by the CIDEP and CIDNP mechanisms, large-scale computer simulations have often been carried out [2–4]. However, as the present attentions are focused on behavior of the radical pairs and polarization of free radicals, the magnitude of discrete SLE dimension is limited to 6. The closest inter-radical distance within radical pair is set to d = 0.4 nm, and the distance step Δr is taken to be 0.1 nm. An exponentially decayed exchange interaction is employed by using the following usual formula,

$$J(r) = J_0\exp\left[-\lambda(r-d)\right]. \quad (11)$$

General parameters, J_0 = −100 MHz and λ = 26 nm^{-1} are used. These give $J(r)$ = −2.3 × 10^{-4} MHz at the most apart distance in this work.

The author writes the diffusion super operator in Eq. (8) in a matrix form according to the finite difference technique [2–4] as follows:

$$D\frac{\partial^2\hat{\rho}(r,t)}{\partial r^2} \rightarrow \mathbf{W}\hat{\boldsymbol{\rho}}(t), \quad (12)$$

$$\begin{array}{cc} & r/\mathrm{nm} = \begin{array}{cccccc} 0.4, & 0.5, & 0.6, & 0.7, & 0.8, & 0.9 \end{array} \\ \mathbf{W} = \dfrac{D}{\Delta r^2} & \begin{pmatrix} -2\left[1+(\Delta r/d)\right] & +2 & & & & \\ 1 & -2 & 1 & & & \\ & 1 & -2 & 1 & & \\ & & 1 & -2 & 1 & \\ & & & 1 & -2 & 0 \\ & & & & 2 & 0 \end{pmatrix} \end{array} \quad (13)$$

Here, $\hat{\boldsymbol{\rho}}(t)$ is a density operator vector also spanned by the inter-radical distance r. In Eq. (12), notes of the spin states are omitted.

The Hamiltonian commutator super operator in Eq. (7) is written in the Liouville space by using the exchange interaction expressed in Eq. (11). Additionally, the diffusion super operator depicted in Eq. (13) and the relaxation super operator expressed in Eq. (10) are superimposed so as to form a stochastic Liouville super operator **L**. Then the super operator **L** is spanned by the electron spin Liouville space and by the inter-radical distance r, making $\hat{\boldsymbol{\rho}}(t)$ evolve as

$$\frac{\partial\hat{\boldsymbol{\rho}}(t)}{\partial t} = \mathbf{L}\hat{\boldsymbol{\rho}}(t). \tag{14}$$

Thus it is ready to calculate the inter-radical distance-dependent time evolution of the spin system. At a glance of SLE, the super operators contain imaginary values, and the diffusion super operator is not symmetric. As a consequence, the stochastic Liouville super operator is not Hermitian and diagonalization techniques cannot be utilized. Therefore, in the present study, a small time increment method is employed in order to obtain the FT-EPR signals. Namely, the formal solution of SLE with the stochastic Liouville super operator $\mathbf{L}$ is expressed from Eq. (14) as

$$\hat{\boldsymbol{\rho}}(t) = \exp(\mathbf{L}t)\hat{\boldsymbol{\rho}}(0), \tag{15}$$

and the exponential operator is extended by a small time increment Δt to the 2nd-order, giving

$$\exp(\mathbf{L}\Delta t) \cong \mathbf{1} + \mathbf{L}\Delta t + \frac{1}{2}\mathbf{L}^2\Delta t^2. \tag{16}$$

In the present calculations, Δt = 0.2 ns is adequate from the points of view of both the calculation speed of a computer and convergency of the results.

The chemical reaction from the photo-excited triplet precursor is taken into consideration by means of the formation of the elements of the density operator of the radical spin at the closest inter-radical distance d and of the decay of the density operator in the 1st order with the rate constant k. Namely, the formation of the spin density operator is expressed by

$$\rho(r=d, t+\Delta t)_{T_jT_j} = \rho(r=d,t)_{T_jT_j} + k\Delta t\sigma(t)_{T_jT_j}, \quad j=\pm,0, \tag{17}$$

and the decay of the density operator of the triplet precursor is expressed by:

$$\sigma(t+\Delta t)_{T_jT_j} = \sigma(t)_{T_jT_j} - k\Delta t\sigma(t)_{T_jT_j}, \quad j=\pm,0, \tag{18}$$

where $\sigma(t)_{T_+T_+}$, etc., are the elements of the density operator of the triplet precursor, and the initial triplet-state density operator is taken to be

$$\sigma(t=0)_{T_jT_j} = \frac{1}{3}, \quad j=\pm,0. \tag{19}$$

The differential increments of the density operators are also taken into consideration in the time evolution of the density operator of radical pairs.

In a single-microwave pulse FT-EPR experiment with delay time from the laser pulse of τ and with duration of the microwave pulse of t_1, the density operator at t_2 after the microwave pulse is expressed by using the formal integration as

$$\hat{\boldsymbol{\rho}}(\tau,t_1,t_2) = \exp(\mathbf{L_0}t_2)\exp(\mathbf{L_1}t_1)\exp(\mathbf{L_0}\tau)\hat{\boldsymbol{\rho}}(0). \tag{20}$$

Here,

$$-\mathrm{i}[H_0(r)_{\mathrm{rot}}, \hat{\rho}(r.,t)] + D\Gamma_r(r)\hat{\rho}(r,t) + R\hat{\rho}(r,t) \to \mathbf{L_0}\hat{\boldsymbol{\rho}}(t), \tag{21}$$

$$-\mathrm{i}[H_0(r)_{\mathrm{rot}} + H_{1,\mathrm{rot}}, \hat{\rho}(r,t)] + D\Gamma_r(r)\hat{\rho}(r,t) + R\hat{\rho}(r,t) \to \mathbf{L_1}\hat{\boldsymbol{\rho}}(t). \tag{22}$$

The spin density operator $\rho(r,\tau,t_1,t_2)$ is calculated from the density operator vector $\hat{\boldsymbol{\rho}}(t)$ by using the corresponding inter-radical distance. The FID signal $s_+(\tau,t_1,t_2)$ should then be written as follows:

$$s_+(\tau,t_1,t_2) = \int_{r=d}^{\infty} r^2\mathrm{tr}\{(S_x+\mathrm{i}S_y)\rho(r,\tau,t_1,t_2)\}\,\mathrm{d}r. \tag{23}$$

The FID signal originally written by Eq. (23) includes transverse magnetization of the both the radical pairs and free radicals at all distances of $r \geqslant d$. These transverse magnetization contains contribution from the radical pairs with large absolute values of $J(r)$. Such radical pairs are supposed to give broad line width signals due to the rapid transverse relaxation, and hence their FID signals are probably thought to decay within the instrumental deadtime. Furthermore, the SLE (6) does not include relaxation phenomena such as dipolar–dipolar relaxation, fluctuations of orientation-dependent exchange interactions, and so on. These phenomena are eliminated by utilizing magnetization of only radical pairs with the inter-radical distance of $\geqslant$0.7 nm. Since the most apart inter-radical distance is taken to be 0.9 nm, the FID signal $S_+(\tau,t_1,t_2)$ discussed in this article is expressed as

$$S_+(\tau,t_1,t_2) \propto \sum_{r=0.7\mathrm{nm}}^{0.9\mathrm{nm}} r^2\mathrm{tr}\{(S_x+\mathrm{i}S_y)\rho(r,\tau,t_1,t_2)\}\Delta r, \tag{24}$$

where Δr is taken to be 0.1 nm as in Eq. (13).

The inter-radical distance of 0.7 nm corresponds to J = −0.042 MHz. It should be noticed that taking the inter-radical distance from 0.7 to 0.9 nm in calculation of the FID does not mean usage of some average exchange interaction models, but does consider simultaneously large absolute values of exchange interactions within the full range cited in Eq. (13) in the course of time evolution of the spin system.

3.1. The simulations of 1D FT-EPR spectra

In the simulations, the delay times from laser flash τ are varied and the microwave pulse duration t_1 is fixed constant. The 1D FIDs along t_2 are calculated by Eq. (24) with 256 steps of 10 ns. The FIDs are apodized with the Hanning windows, and zerofilled to 1024 points, and the successive Fourier transformations give 1D FT-EPR spectra. Parameters used here are tabulated in Table 1.

3.2. The calculations of free radical polarization due to ST_0 mixing RPM

The RPM polarizations are discussed by utilizing the bases of (S,T_0) in the Hilbert space at first, and then the discussion is transferred to the Liouville space. The numerical calculations are made by the use of the SLE concerning about $|S\rangle$ and $|T_0\rangle$ bases.

The EPR polarization of spin a is expressed as

$$P_a(t) = -2\mathrm{tr}\{\rho(t)S_{az}\}. \tag{25}$$

This polarization takes positive value for the EPR absorption, and negative for emission.

Here,

$$2S_{az} = (S_{az} - S_{bz}) + (S_{az} + S_{bz}), \tag{26}$$

and the 2nd term in Eq. (26) becomes zero matrix in the Hilbert space spanned by $|S\rangle$ and $|T_0\rangle$. The 1st term becomes

$$\begin{matrix} & |S\rangle & |T_0\rangle \end{matrix}$$

$$S_{az} - S_{bz} = \begin{bmatrix} 0 & 1 \\ 1 & 0 \end{bmatrix} \tag{27}$$

Hence the polarization is expressed by

Table 1
Parameters used in the simulation displayed in Fig. 1

Name of parameter	Physical quantity
Frequency of the center of the spectrum	−1.46 MHz
$g_a = g_b$	2.0037
$a(CD_3)$[a]	8.2 MHz
$a(OD)$[a]	0.33 MHz
B_1	0.89 mT
Duration of the microwave pulse, t_1	10 ns
T_1	2 μs
T_2	1 μs
Diffusion coefficient, D	0.2 m^2 MHz
Reaction rate from the triplet precursor, k	0.2 μs^{-1}

[a] Hyperfine coupling constant.

$$P_a(t) = -\{\rho_{ST_0}(t) + \rho_{T_0S}(t)\}. \quad (28)$$

Time evolution of the statistical spin system is obtained by the SLE expressed by Eq. (6) and in the same manner as described in the simulation method. The same parameters for diffusion, relaxation and rising rate constant are used as in the simulation calculations of the 1D FT-EPR spectra. Additionally, several different diffusion coefficients are also used to examine the signal rising and decay processes. The density operator elements for the most apart inter-radical distance, $r = 0.9$ nm, are regarded as those for free radicals. Delay time τ from laser flash is varied in Eq. (20). The polarization is calculated according to Eq. (27).

3.3. The simulations of 2D FT-EPR nutation spectra

In the simulations of 2D FT-EPR nutation spectra, Eq. (24) is used with the fixed delay time τ from the laser flash and the microwave pulse time t_1 varying by 64 points of 8 ns. The successive FIDs along t_2 are calculated with 128 steps of 10 ns. The 2D FIDs are apodized with the Hanning windows in the both dimensions, and zerofilled to 128×256 complex matrices. The 2D Fourier transformations of 2D FIDs give 2D FT-EPR spectra that are depicted in the absolute value representations with the nutation frequencies $f1$ and EPR frequencies $f2$. Parameters utilized there are listed in Table 2.

4. Results and discussion

4.1. The overview of 1D FT-EPR spectra

Several diffusion coefficients were examined in the simulation processes, and rising of the antiphase structures and free radical CIDEP signals were found to be well simulated when it was set to $D = 0.2$ nm^2 MHz. The rising rate constant from the triplet precursor was also found to be $k = 0.2$ μs^{-1}.

Fig. 1 displayed calculated 1D FT-EPR spectra. The microwave pulse was settled to have the duration t_1 of 10 ns and the strength B_1 of 0.89 mT. The phase corrections were made according to the off-resonance effects of free radicals under this microwave pulse excitation. In Fig. 1, remarkable antiphase Emission/Absorption (E/A)-like or dispersive-like patterns strongly appeared around the centers of the spectra, that were attributed to the radical pairs themselves. The line shapes of these signals were discussed below. The other emission and absorption signals were ascribed to the free radical CIDEP due to the ST_0 mixing RPM. It was also demonstrated that the intensity ratios of EPR signals for the both species observed in the experiment [12] were well simulated by the calculation.

The EPR excitation pulse condition in the spectra of Fig. 1 corresponded to ca. $\pi/2$ pulses in the on-resonance positions. The 1D FT-EPR spectra previously reported in Ref. [12] were concluded to be

Table 2
Parameters used in the simulation displayed in Fig. 6

Name of parameter	Physical quantity
Frequency of the center of the spectrum	−1.25 MHz
$g_a = g_b$	2.0037
$a(CD_3)$[a]	8.2 MHz
$a(OD)$[a]	Abbreviated
B_1	0.55 mT
Duration of the microwave pulse, t_1	Varied
T_1	2 μs
T_2	1 μs
Diffusion coefficient, D	0.2 nm^2 MHz
Reaction rate from the triplet precursor, k	0.2 μs^{-1}

[a] Hyperfine coupling constant.

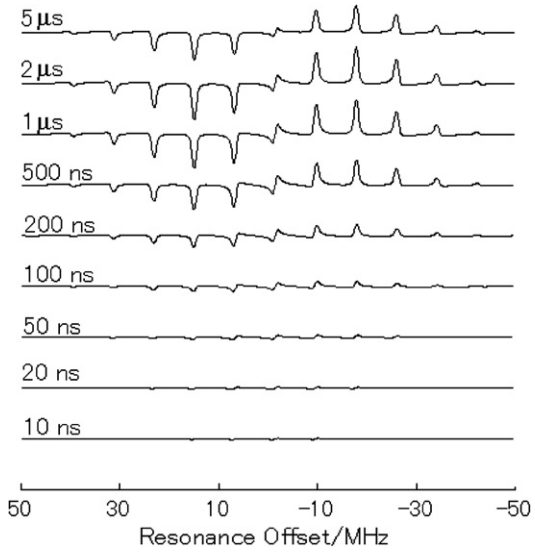

Fig. 1. Simulations of 1D FT-EPR spectra of photo-chemically generated radical pairs and free radicals of deuterated acetone in 2-propanol system. The times displayed upper the each spectrum indicated delay times after laser excitation.

obtained under ca. $\pi/2$ microwave excitation pulse. A theory developed by Kroll et al. [8] suggested that FT-EPR signals of radical pairs themselves would not be observed by the $\pi/2$ pulse. The theory [8] on flip angle dependencies of signal intensities of the radical pairs different from those of free radicals in the FT-EPR experiments were able to be understood in terms of the product operator formalism [24] used in the theory of 2D NMR. That is to say, magnetizations of longitudinal two spin order led to such flip angle dependencies. However the present author's analyses [11–14], including the off-resonance effect, demonstrated clearly that radical pair signals appeared even if the flip angle of microwave pulse was $\pi/2$. This phenomenon would be attributed to the off-resonance effect of coupling partner spins.

4.2. The 1D FT-EPR line shape problems of the radical pair signals

In the field of CW TR-EPR, antiphase structures of the EPR line shapes were attributed to radical pairs themselves. At early stages of the studies [1], the antiphase structures were interpreted in terms of quasi-static average exchange interaction model, where each resonance line was split by the absolute value of the twice of exchange interaction, i.e., $|2J|$. In the course of theoretical studies on the antiphase structure problems, some remarkable discussions have been developed. Shushin supposed a simple Bloch-type equation model by sudden perturbation approximation [25]. Tarasov et al. demonstrated an SLE treatment that included the radical pair themselves as well as free radical CIDEPs [5].

Furthermore, significant progresses [6,7] have been brought by Neufeld and Pedersen. These theories showed that the transverse magnetizations created by the EPR excitations and the diffusion processes were essential for the antiphase structures of the radical pairs systems. According to these theories, one could easily think that the excitation microwaves pulses in the FT-EPR experiments played central roles to produce the antiphase structures. In addition, the effects of diffusion within the radical pairs simultaneously had a crucial part. Although there were differences between CW and FT methods, it was the most important point that the roles of both of the excitation microwave pulse and the fluctuation of the exchange interactions within the radical pairs were substantial. Additionally, FT-EPR experiments for the radical pairs were made on the non-equilibrated coupled spin states, and possibilities of

estrangements between CW and FT methods might arise as well known in the field of NMR [24].

The line shape caused by the radical pairs was observed to be dispersive for the case of short lived them in the field of FT-EPR [8]. However, for the long-lived radical pairs, the FT-EPR line shape problem has not still been solved, yet.

Therefore, the author displayed simply the line shape of the radical pairs obtained by the SLE calculations under the same experimental condition as described in the previous papers [12]. The dependence of the EPR line shape on the microwave excitation pulses would be treated in the session of the 2D FT-EPR nutation spectra. Expanded display of the central part of the spectrum of Fig. 1 was shown in Fig. 2. The antiphase *E*/*A*-like or dispersive-like pattern could be assigned to signals of the radical pairs.

In the previous report [12] the value of −0.56 MHz was adopted for simulation as the averaged exchanged interaction based on the observed line split, because the split might simply be estimated to be 2×0.56 MHz in the 1D FT-EPR experiment. However, in this article the author applied not any average exchange interaction models, but the SLE modeling. In order to discuss the line shapes, one should necessarily know how the FT-EPR signals depended on the microwave excitation pulses.

4.3. The rising and decay of FT-EPR signals of the radical pairs

One of the greatest capabilities of FT-EPR was to be able to observe the rising behavior of the EPR signals. Fig. 3 showed the FT-EPR intensity changes of the radical pair signals in the central part of the simulated spectra with different delay times from the laser flash. The calculated spectra included hyperfine couplings with the deuterated hydroxyl group. This figure also displayed a nonlinear least square double exponential fitting of the rising and decay phenomena.

The rising and decay pattern were well fitted by the double exponential formula. The rising and decay rate constants were calculated to be 3.73 and 0.258 μs^{-1}, respectively. The former was much faster than the rising rate from the triplet precursors of 0.2 μs^{-1}. This meant that rising of the antiphase structures could not simply be accounted in terms of only the reaction rate of triplet precursor, and that spin dynamics mechanism yielding the radical pair signals was more important. This finding could be related to the suggestions of Refs. [6,7]. The latter rate constant was slower than the inverse of the relaxation times. This fact implied that not only phenomenological relaxations but also spin dynamics including diffusions of the pairs had also crucial roles.

Detailed discussion was needed, because the diffusions of the radical pairs and the spin relaxations should be taken into considerations simultaneously when the spin polarizations were accounted.

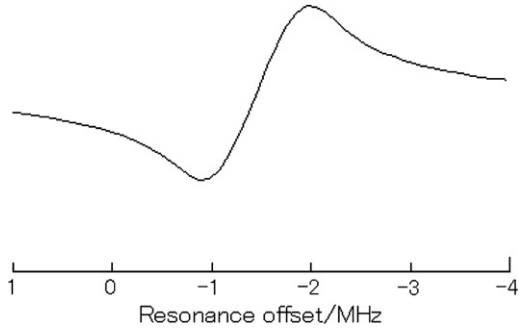

Fig. 2. Central parts of the FT-EPR spectrum with delay time from the laser flash of 500 ns in Fig. 1 calculated by means of SLE.

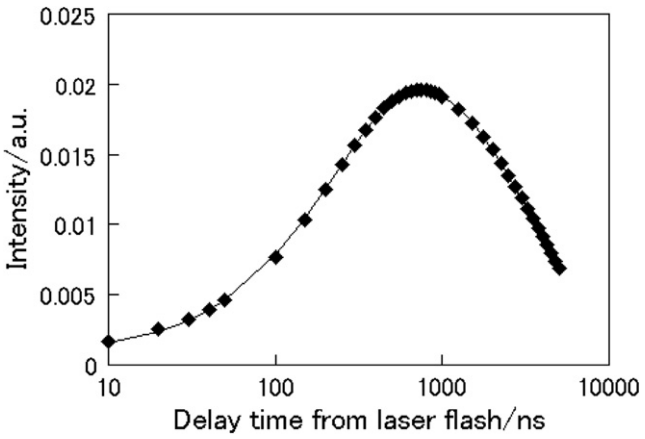

Fig. 3. Rising and decay of intensities of FT-EPR signals of the radical pairs themselves and their fittings by a nonlinear least-square double-exponential pattern. Dotted points displayed the intensities obtained by the SLE simulations, and the curve meant the double-exponential fitting. The radical pairs antiphase structure signal intensities were well reproduced by this formula.

4.4. The rising of polarization due to ST_0 mixing RPM

By the use of SLE, rising of the electron spin polarization due to the ST_0 mixing RPM could be simulated. Fig. 4 showed the rising and decay of the ST_0 RPM polarization for each hyperfine line under the same diffusion and relaxation parameter as those described in Section 1. Although Shushin [22,23] has suggested that some deviations from the classical Adrian's model [21] would exist, the rising behaviors of the ST_0 mixing RPM CIDEP have not been clarified, yet. Fig. 5(a–d) depicted the early stages of rising of spin polarization obtained with several different diffusion coefficients. In the simulation, the hyperfine couplings with the hydroxyl group were neglected. These figures clearly showed that rising of the spin polarizations was not exponential under slow diffusion, whereas the rising became exponential when diffusion was fast.

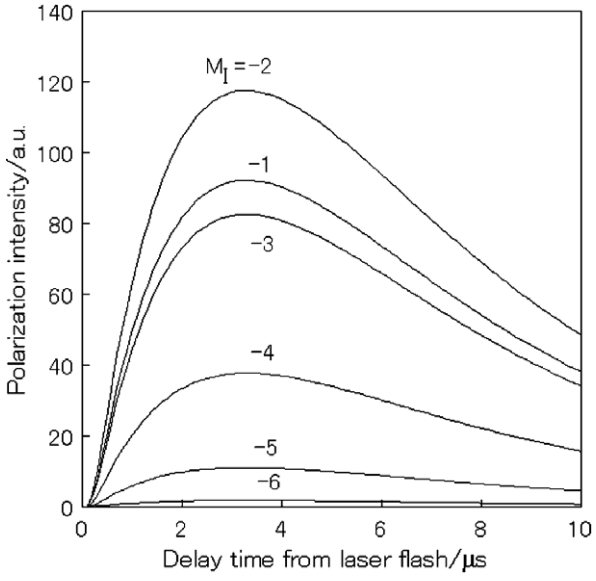

Fig. 4. Rising and decay of spin polarization due to ST_0 mixing RPM in deuterated acetone and 2-propanol system. The M_Is indicated the spin states of the methyl group (CD_3).

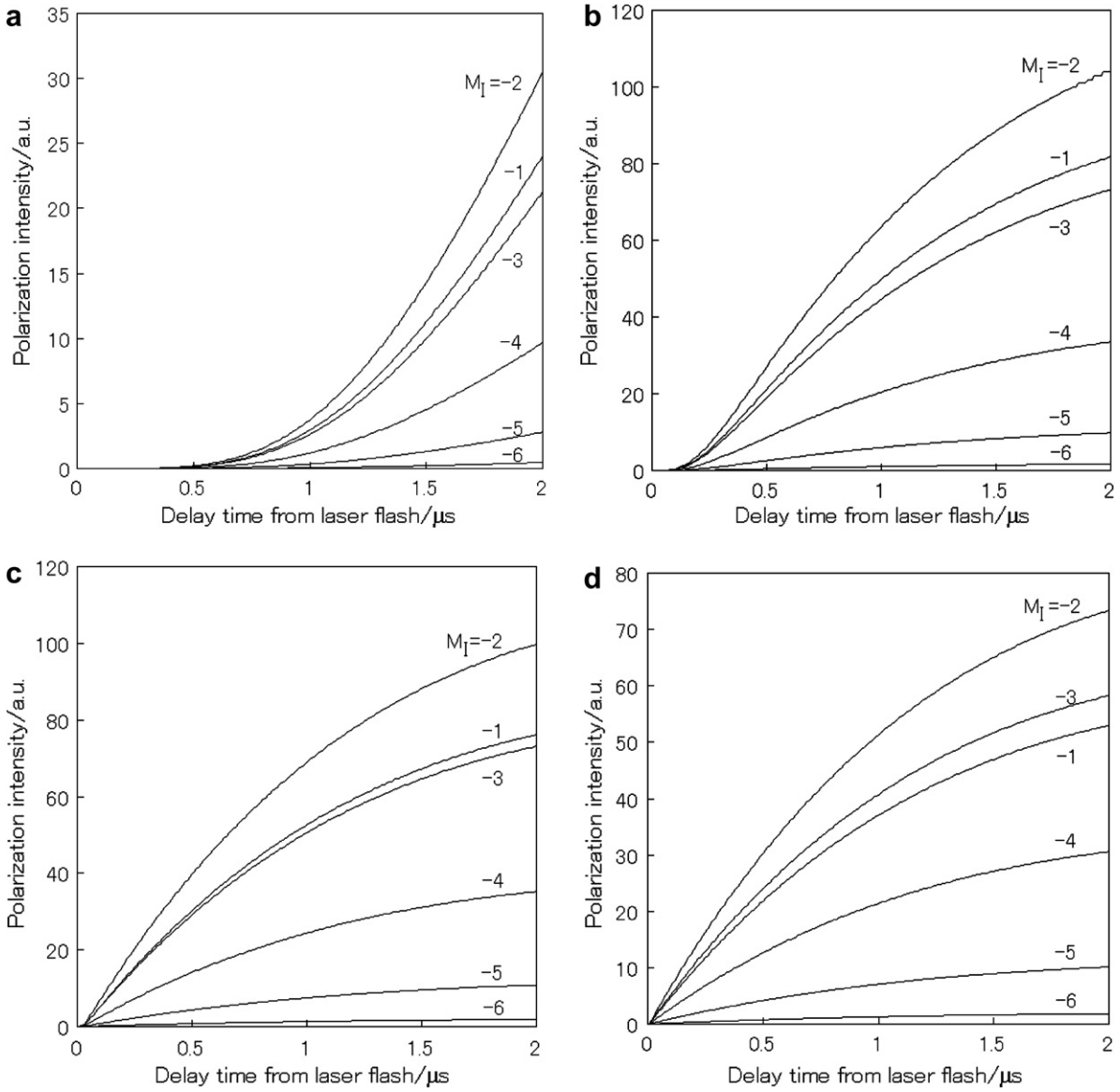

Fig. 5. The early time region of rising of spin polarization owing to ST_0 mixing RPM under different diffusion coefficients: D/(nm^2 MHz) = 0.02 in (a), 0.2 in (b), 2 in (c) and 20 for (d). Rinsing profiles deviated considerably from exponential under slow-diffusion conditions.

4.5. The 2D FT-EPR nutation spectra

2D FT-EPR spectra were simulated for the two cases of the different delay times τ from laser flash. One was for τ = 400 ns and the other was for τ = 5 μs. In the former the radical pair signals were relatively strong, while in the latter the radical pairs almost disappeared. In these simulations, the hyperfine couplings with the hydroxyl group (OD) were neglected. The simulated 2D FT-EPR nutation spectra were depicted in Fig. 6.

Interpretations of the nutation frequencies of the radical pairs in the 2D FT-EPR nutation spectra, except for the strong DC components in the nutation dimension, were fully described in the previous paper [12]. It should be emphasized here that a single SLE with different delay times from the laser flash gave the different 2D FT-EPR nutation spectra.

In the simulation described here, 2D FT-EPR spectra showed considerably strong DC nutation peaks, that were actually observed in the experiments. These strong DC components were not expected from the theoretical analysis for nutation of radical pairs cited in Ref [12]. As one possible origin of these DC components, the spin relaxation during the EPR microwave pulse would be considered. The effects of spin relaxations during the microwave pulse in the nutation experiment have already been pointed out for the spin quartet states in solution by Ohba et al. [26].

Fig. 7(a–d) displayed stack plots of simulated 2D FT-EPR nutation spectra for simple radical pair model cases with the resonance offset combination of 10 and −10 MHz under different delay times from laser flash and under different relaxation times. DC nutation frequencies appeared more largely as the relaxation times were shorter in the both cases with different delay times. Therefore the main reason for the appearance of the strong DC nutation components would be ascribed to spin relaxation during the microwave excitation pulse.

It was also postulated that some further developments of spin polarization during the microwave pulse would cause the DC nutation components. This possibility was however easily denied, since the strength of the DC components and nutation peaks at ca.

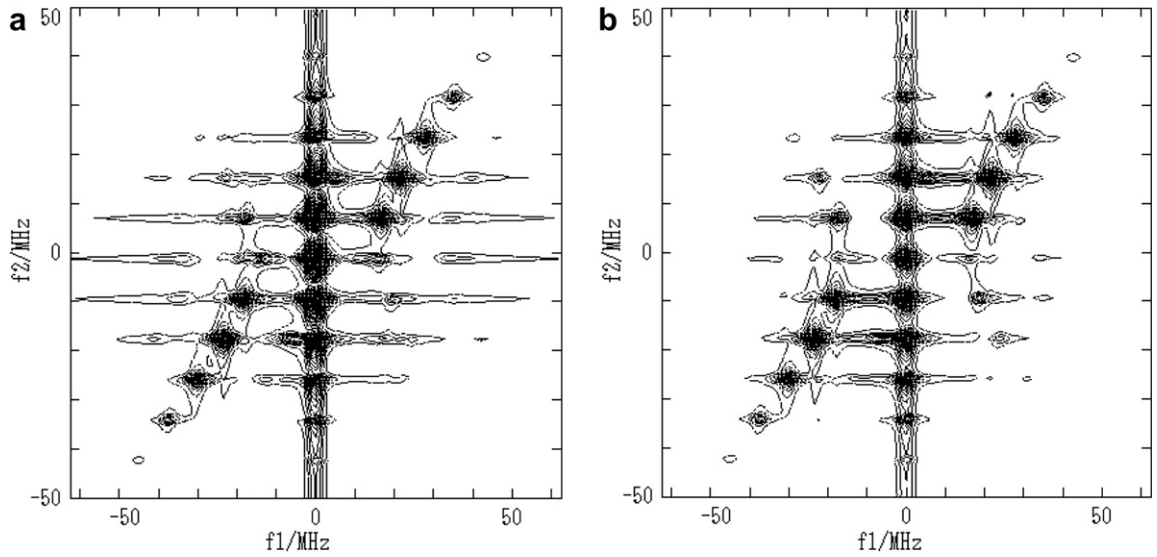

Fig. 6. Simulations of 2D FT-EPR nutation spectra with two different delay times from laser flash, $\tau = 400$ ns in (a) and 5 μs in (b). In the former delay time, the radical pair signals were relatively strong, but the signals almost disappeared in the latter. The spectra (a) and (b) were drawn in the same scale.

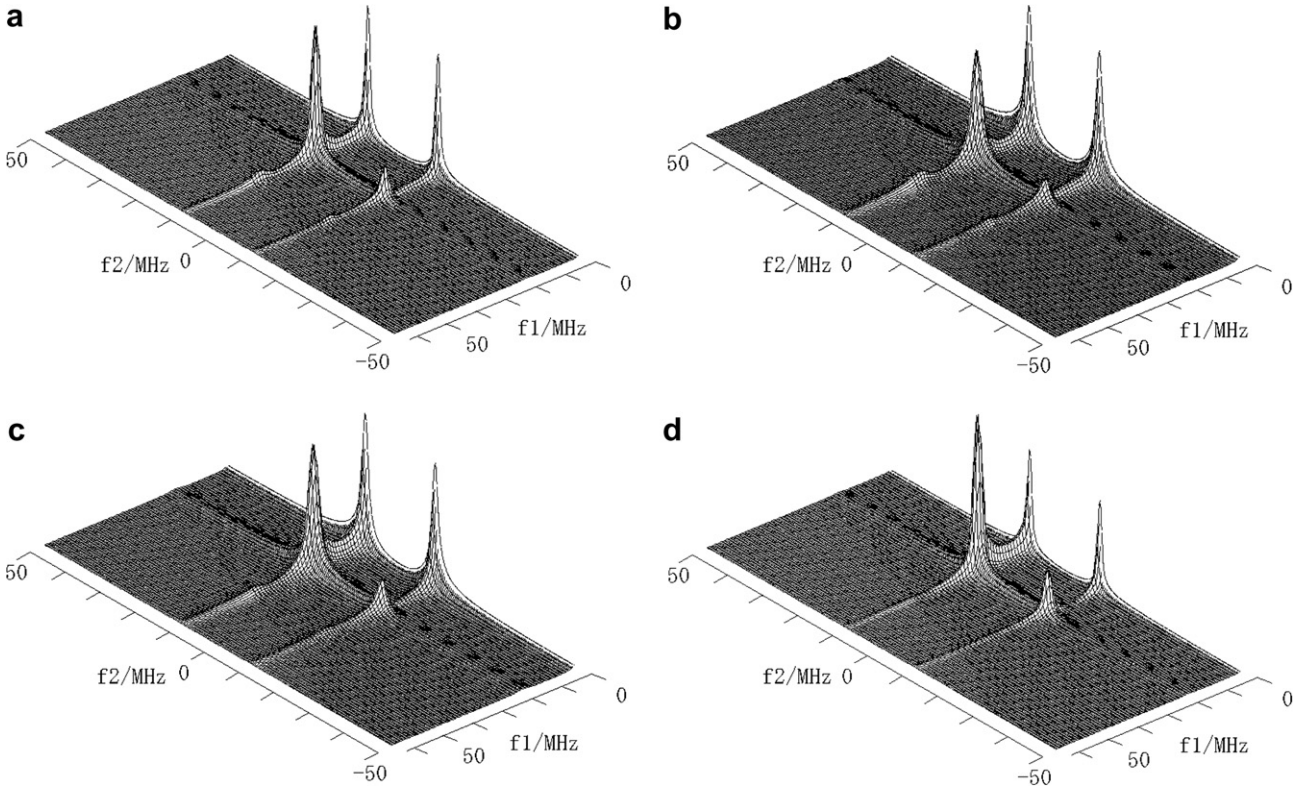

Fig. 7. Simulations of 2D FT-EPR nutation spectra of a simple model radical pair system with the resonance offset of 10 MHz and −10 MHz under two different delay times τ from laser flash and two different relaxation times (T_1 and T_2). $\tau = 400$ ns in (a) and (b) and $\tau = 5$ μs in (c) and (d). $T_1 = 1$ μs and $T_2 = 0.5$ μs in (a) and (c), and $T_1 = 20$ μs and $T_2 = 10$ μs in (b) and (d). Fast spin relaxation made the DC nutation components strong. The strengths of nutation peak with the frequencies of ca. 20 MHz and DC components were almost comparable in (a) and (c). This implied that effects of further developments of spin polarization during microwave excitation pulse were relatively small.

20 MHz are not little affected by using different delay times of 400 ns and 5 μs, as depicted in Fig. 7(a–d).

In the present simulation calculations for the 2D FT-EPR nutation spectra, the line widths in the nutation dimensions were also well reproduced. In the previous simulation [12] using an averaged and constant exchange interaction value, the line width along the nutation axes could not be given straightforwardly. The present study could estimate the line width correctly by the use of the super operator in terms of diffusion and phenomenological relaxation.

The line shape theories on CW TR-EPR spectra of the radical pairs proposed by Neufeld and Pedersen [6,7] demonstrated the importance of the effects of excitation microwave. The aforementioned 2D nutation method and the simulations would supplement information to the 1D technique and simulation results.

5. Conclusions

SLEs were solved so as to simulate 1D and 2D FT-EPR spectra containing radical pairs as well as their dissociated free radicals polarized by the ST_0 mixing RPM.

Through the simulation calculations of delay time dependence and the EPR line shape of 1D FT-EPR spectra, an adequate diffusion coefficient and a reaction rate from the triplet precursor were determined. The simulated 1D FT-EPR spectra showed good agreement with the experimental ones.

Next, tried were simulations of delay time dependences of the ST_0 mixing RPM CIDEP of the free radicals. The rising and decay of the signals were well demonstrated, and in the very early stage the rising of the RPM CIDEP showed appreciable deviation from exponential behavior.

Finally, the author succeeded in the simulation of the 2D FT-EPR nutation spectra with and without radical pairs by a single SLE. The experimentally observed significant DC nutation frequencies were also simulated and the existence was ascribed to be due to the spin relaxation effects during the microwave excitation pulse. The line width along the nutation axes were also simulated straightforwardly by use of the super operators of the diffusion and phenomenological relaxation.

Acknowledgment

The author thanks Professor emeritus Masamoto Iwaizumi of Tohoku University for his encouragement and instructive discussions about this study.

References

[1] S. Nagakura, H. Hayashi, T. Azumi (Eds.), Dynamic Spin Chemistry Magnetic Controls and Spin Dynamics of Chemical Reactions, Kodansha and Wiley, Tokyo, 1998.
[2] J.B. Pedersen, J.H. Freed, J. Chem. Phys. 58 (1973) 2746–2762.
[3] J.B. Pedersen, J.H. Freed, J. Chem. Phys. 59 (1973) 2869–2885.
[4] J.H. Freed, J.B. Pedersen, Adv. Magn. Reson. 8 (1976) 1–84.
[5] V.F. Tarasov, H. Yashiro, K. Maeda, T. Azumi, I.A. Shkrob, Chem. Phys. 212 (1996) 353–361.
[6] A.A. Neufeld, J.B. Pedersen, J. Chem. Phys. 109 (1998) 8743–8746.
[7] A.A. Neufeld, J.B. Pedersen, J. Chem. Phys. 113 (2000) 1595–1604.
[8] G. Kroll, M. Pluscau, K.-P. Dinse, H. van Willigen, J. Chem. Phys. 93 (1990) 8709–8716.
[9] P.R. Levstein, H. van Willigen, J. Chem. Phys. 95 (1991) 900–907.
[10] P.R. Levstein, H. van Willigen, Chem. Phys. Lett. 187 (1991) 415–422.
[11] R. Hanaishi, Y. Ohba, K. Akiyama, S. Yamauchi, M. Iwaizumi, J. Chem. Phys. 103 (1995) 4819–4822.
[12] R. Hanaishi, Y. Ohba, K. Akiyama, S. Yamauchi, M. Iwaizumi, J. Magn. Reson. A 116 (1995) 196–205.
[13] R. Hanaishi, Y. Ohba, S. Yamauchi, M. Iwaizumi, Bull. Chem. Soc. Jpn. 69 (1996) 1533–1541.
[14] R. Hanaishi, K. Yamamoto, Y. Ohba, S. Yamauchi, M. Iwaizumi, Appl. Magn. Reson. 10 (1996) 55–69.
[15] K. Tominaga, S. Yamauchi, N. Hirota, Chem. Phys. Lett. 149 (1988) 32–36.
[16] K. Tominaga, S. yamauchi, N. Hirota, J. Chem. Phys. 92 (1990) 5175–5185.
[17] K. Tominaga, S. Yamauchi, N. Hirota, J. Chem. Phys. 88 (1987) 553–562.
[18] S.K. Wong, T.M. Chui, J.R. Bolton, J. Phys. Chem. 85 (1981) 12–14.
[19] S. Basu, A.J. Grant, K.A. McLauchlan, Chem. Phys. Lett. 94 (1983) 517–521.
[20] M.C. Thurnauer, T.M. Chui, A.D. Trifunac, Chem. Phys. Lett. 116 (1985) 543–547.
[21] F. Adrain, L. Monchick, J. Chem. Phys. 71 (1979) 2600–2610.
[22] A.I. Shushin, Chem. Phys. 144 (1990) 201–222.
[23] A.I. Shushin, Chem. Phys. Lett. 170 (1990) 78–88.
[24] R.R. Ernst, G. Bodenhausen, A. Wokaun (Eds.), Principles of Nuclear Magnetic Resonance in One and Two Dimensions, Oxford, New York, 1985.
[25] A.I. Shushin, Chem. Phys. Lett. 245 (1995) 183–188.
[26] Y. Ohba, N. Mizuochi, S. Yamauchi, Appl. Magn. Reson. 14 (1998) 217–234.